Excerpt from the Proceedings of the 2011 COMSOL Conference in Boston

Planar Geometry Ferrofluid Flows in Spatially Uniform Sinusoidally Time-varying Magnetic Fields

Shahriar Khushrushahi[*1], Alexander Weddemann[1], Young Sun Kim[1] and Markus Zahn[1]
[1]Massachusetts Institute of Technology,
*Corresponding author: 77 Massachusetts Avenue 10-174, Cambridge, MA 02139, shahriar@alum.mit.edu

Abstract: Past work [1-5] has analyzed ferrofluid flows subjected to magnetic fields in spherical and cylindrical geometries, using COMSOL Multiphysics. However, ferrofluid flows in the planar case, having analytical solutions, is usually the stepping stone to understanding flows in more complicated geometries. The reason is that under a uniform magnetic field, the ferrofluid's magnetization depends only on the particle spin velocity and not the fluid velocity. In addition, the uniform magnetic field results in zero magnetization force densities along the duct axis.

The case of planar Poiseuille ferrofluid flows in planar ducts, stressed by uniform sinusoidally applied magnetic fields transverse and parallel to the duct axis, has been previously analyzed [6-10] using Mathematica as the software of choice. This work describes how to solve the previously solved planar geometry cases using COMSOL Multiphysics. The results obtained replicate those obtained using Mathematica.

Keywords: ferrofluids, ferrohydrodynamics, uniform magnetic fields, planar geometry, spin diffusion, Poiseuille flows

1. Introduction

Ferrofluids are stable colloidal suspensions of single-domain surfactant coated ferro- or ferrimagnetic nanoparticles in a carrier fluid. Ferrofluids exhibit superparamagnetism and have a typical magnetic volume fraction of 10%.

The nanoparticles have typical diameters of order 10 nm with a 1-2 nm surfactant coated layer. This small size prevents them from agglomerating under gravity and allows for easy dispersion due to Brownian motion. The surfactant layer prevents the nanoparticles from agglomerating under van der Waals and magnetic attraction forces.

The application of AC magnetic fields to ferrofluids tends to orient the magnetic moments of the constituting magnetic particles in the direction of the applied field with resistance to free rotation of the particles from fluid viscosity or magnetic crystalline anisotropy [4]. This causes the ferrofluid magnetization $\boldsymbol{M}$ to lag behind the applied magnetic field $\boldsymbol{H}$ resulting in a body torque density acting on the ferrofluid. Ferrohydrodynamic equations account for this antisymmetric stress when $\boldsymbol{M}$ and $\boldsymbol{H}$ are not collinear while satisfying linear and angular momentum conservation for the ferrofluid [6, 11].

2. Planar Geometry Setup

Figure 1 illustrates the planar duct containing the ferrofluid. To impose the horizontal tangential field H_z, ±y directed surface currents on the x=0 and x=d planes are required. The uniform AC magnetic flux density B_x is imposed by an external permanent magnet or electromagnet as shown in Figure 2.

Poiseuille flow is generated by applying a pressure difference in the z direction and hence the flow velocity can only be in that direction. The spin velocity $\boldsymbol{\omega}$ is assumed to be in the y direction. Since the planar duct does not vary in the y or z directions, both $\mathbf{v}$ and $\boldsymbol{\omega}$ can only vary with the x coordinate.

$$\mathbf{v} = v_z(x)\mathbf{i_z}, \boldsymbol{\omega} = \omega_y(x)\mathbf{i_y} \quad (1)$$

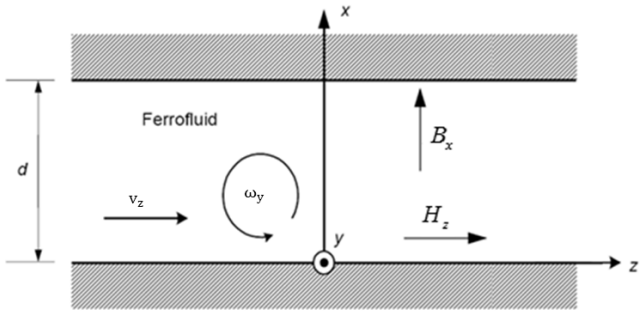

Figure 1. Planar ferrofluid layer between rigid walls. Planar Poiseuille flow is generated by applying a pressure difference between the inlet and outlet. It is magnetically stressed by a uniform x directed AC magnetic flux density B_x, or by a uniform z directed tangential AC magnetic field H_z [4, 6, 7].

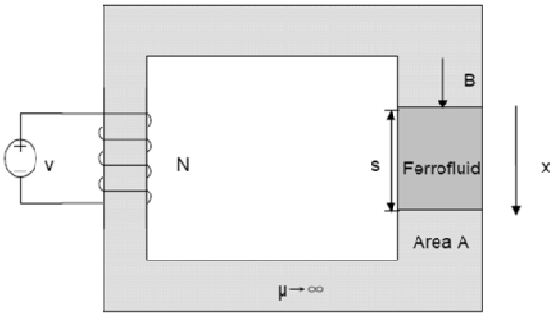

Figure 2. An imposed voltage source will impose a flux in the magnetic circuit, that will result in a flux density **B** that is spatially uniform in the ferrofluid [4, 7].

3. Governing Equations

3.1 Ferrohydrodynamics

The conservation of linear and angular momentum equations [11] are given in Eq. 2 and Eq. 3.

$$\rho\left[\frac{\partial \mathbf{v}}{\partial t}+(\mathbf{v}\cdot\boldsymbol{\nabla})\mathbf{v}\right]=-\boldsymbol{\nabla}p+2\zeta\boldsymbol{\nabla}\times\boldsymbol{\omega}+(\zeta+\eta)\boldsymbol{\nabla}^2\mathbf{v}+\mathbf{F}-\rho\mathbf{g}\mathbf{i}_\mathbf{x} \quad (2)$$

$$I\left[\frac{\partial \boldsymbol{\omega}}{\partial t}+(\mathbf{v}\cdot\boldsymbol{\nabla})\boldsymbol{\omega}\right]=\mathbf{T}+2\,\zeta(\boldsymbol{\nabla}\times\mathbf{v}-2\boldsymbol{\omega})+\eta'\boldsymbol{\nabla}^2\boldsymbol{\omega} \quad (3)$$

where the variables are dynamic pressure p [N/m^2], gravitational acceleration g [m/s^2], ferrofluid mass density ρ [kg/m^3], fluid moment of inertia density I [kg/m], spin velocity $\boldsymbol{\omega}$ [1/s], magnetic force density $\mathbf{F}$ [N/m^3], torque density $\mathbf{T}$ [N/m^2], ferrofluid dynamic viscosity η [N-s/m^2], vortex viscosity ζ=1.5$\eta\varphi_{vol}$ [N-s/m^2] for small volume fraction φ_{vol} of magnetic nanoparticles [11, 12], and η' [N-s] is the shear coefficient of spin viscosity.

The magnetic force density $\mathbf{F}$ and torque density $\mathbf{T}$ are given as

$$\mathbf{F}=\mu_0(\mathbf{M}\cdot\boldsymbol{\nabla})\mathbf{H} \quad (4)$$

$$\mathbf{T}=\mu_0\mathbf{M}\times\mathbf{H} \quad (5)$$

where $\mu_0=4\pi\times10^{-7}$ [H/m] is the magnetic permeability of free space, $\mathbf{M}$ [A/m] is fluid magnetization and $\mathbf{H}$ [A/m] the magnetic field.

The flow is also assumed to be incompressible $(\nabla\cdot\mathbf{v}=0)$ with no divergence of spin velocity $\boldsymbol{\omega}$ $(\nabla\cdot\boldsymbol{\omega}=0)$. The flow is also assumed to be viscous dominated setting the inertial terms in Eqns 2 & 3 to zero given as

$$\mathbf{0}=-\boldsymbol{\nabla}p+2\zeta\boldsymbol{\nabla}\times\boldsymbol{\omega}+(\zeta+\eta)\boldsymbol{\nabla}^2\mathbf{v}+\mathbf{F}-\rho\mathbf{g}\mathbf{i}_\mathbf{x} \quad (6)$$

$$\mathbf{0}=\mathbf{T}+2\,\zeta(\boldsymbol{\nabla}\times\mathbf{v}-2\boldsymbol{\omega})+\eta'\boldsymbol{\nabla}^2\boldsymbol{\omega} \quad (7)$$

3.2 Magnetization constitutive law

The ferrofluid magnetization relaxation equation derived by Shliomis [12] is

$$\frac{\partial \mathbf{M}}{\partial t}+(\mathbf{v}\cdot\boldsymbol{\nabla})\,\mathbf{M}=\boldsymbol{\omega}\times\mathbf{M}\;-\frac{1}{\tau_{\text{eff}}}(\mathbf{M}-\mathbf{M}_{\text{eq}}) \quad (8)$$

where equilibrium magnetization $\mathbf{M}_{\text{eq}}$ [A/m] is typically given by the Langevin equation.

$$\mathbf{M}_{\text{eq}}=M_s\left[\coth(\beta)-\frac{1}{\beta}\right]\left(\frac{\mathbf{H}}{H}\right),\beta=\frac{M_d V_p \mu_0 H}{kT} \quad (9)$$

with M_s [A/m] the saturation magnetization given as, $M_s=M_d\varphi_{vol}$, M_d = 446 [kA/m] is the domain magnetization for magnetite [11], V_p [m^3] is the magnetic core volume per particle, $\mu_0=4\pi\times10^{-7}$ [H/m] is the magnetic permeability of free space, k=1.38x10^{-23} [J/K] is Boltzmann's constant, T [K] the temperature in Kelvin, and effective relaxation time constant τ_{eff} [s] includes Brownian and Néel effects.

In this analysis, the applied field is assumed not to be strong enough to saturate the fluid and so the equilibrium magnetization $\mathbf{M}_{\text{eq}}$ [A/m] is given as a linear function of magnetic field *inside the ferrofluid* with a slope represented by the magnetic susceptibility of the material χ.

$$\mathbf{M}_{\text{eq}}=\chi\mathbf{H}_{\text{fluid}} \quad (10)$$

3.3 Magnetic Fields

The AC magnetization, flux density and field can be written in phasor form as given as

$$\mathbf{M}=Re\{\hat{\mathbf{M}}e^{-j\Omega t}\},\mathbf{B}=Re\{\hat{\mathbf{B}}e^{-j\Omega t}\},\mathbf{H}=Re\{\hat{\mathbf{H}}e^{-j\Omega t}\} \quad (11)$$

where the small hat symbol above the variables represents the complex amplitude of the individual magnetization, flux density and magnetic field, and Ω represents the AC radian frequency of operation.

The externally imposed magnetic flux density B_x and magnetic field H_z are spatially uniform. This implies that there is no variation in the y and z coordinates and only variation in the x coordinate. Therefore, Gauss's law for magnetic flux density results in a spatially uniform B_x in the ferrofluid volume.

$$\boldsymbol{\nabla}\cdot\mathbf{B}=0\rightarrow\frac{dB_x}{dx}=0\rightarrow B_x=constant \quad (12)$$

Since the ferrofluid is in a current free region Ampere's law results in H_z being constant in the ferrofluid volume.

$$\nabla \times \mathbf{H} = 0 \rightarrow \frac{dH_z}{dx} = 0 \rightarrow H_z = constant \tag{13}$$

The magnetization vectors ($\widehat{M}_x$ and $\widehat{M}_z$) can be solved by substituting the constant H_z and B_x fields into the magnetic relaxation equation of Eq. 8 [4, 6-10] resulting in

$$j\Omega\widehat{M}_x - \omega_y\widehat{M}_z + \frac{\widehat{M}_x}{\tau} = \frac{\chi_0}{\tau}\widehat{H}_x \tag{14}$$

$$j\Omega\widehat{M}_z + \omega_y\widehat{M}_x + \frac{\widehat{M}_z}{\tau} = \frac{\chi_0}{\tau}\widehat{H}_z \tag{15}$$

Using the following relation

$$\hat{B}_x = \mu_0(\hat{H}_x + \hat{M}_x) \rightarrow \hat{H}_x = \frac{\hat{B}_x}{\mu_0} - \hat{M}_x \tag{16}$$

Eqns 14 and 15 result in the following expressions for ($\widehat{M}_x$ and $\widehat{M}_z$)

$$\widehat{M}_x = \frac{\chi_0\left[\hat{H}_z(\omega_y\tau) + (j\Omega\tau + 1)\,\hat{B}_x/\mu_0\right]}{\left[(\omega_y\tau)^2 + (j\Omega\tau + 1)(j\Omega\tau + 1 + \chi_0)\right]} \tag{17}$$

$$\widehat{M}_z = \frac{\chi_0\left[\hat{H}_z(j\Omega\tau + 1 + \chi_0) - \hat{B}_x\omega_y\tau/\mu_0\right]}{\left[(\omega_y\tau)^2 + (j\Omega\tau + 1)(j\Omega\tau + 1 + \chi_0)\right]} \tag{18}$$

It can be seen from Eqns 17 and 18 that $\widehat{M}_x$ and $\widehat{M}_z$ are only a function of spin velocity ω_y which is itself a function of the x coordinate. As a result, H_x and B_z are not spatially uniform due to the magnetization that depends on the x coordinate. Therefore, the total magnetic flux density $\boldsymbol{B}$ and magnetic field $\boldsymbol{H}$ inside the ferrofluid duct are of the form

$$\begin{aligned}\mathbf{B} &= Re\left\{\left[\widehat{\boldsymbol{B}}_x\boldsymbol{i_x} + \widehat{\boldsymbol{B}}_z(x)\boldsymbol{i_z}\right]e^{-j\Omega t}\right\}\\ \mathbf{H} &= Re\left\{\left[\widehat{\boldsymbol{H}}_x(x)\boldsymbol{i_x} + \widehat{\boldsymbol{H}}_z\boldsymbol{i_z}\right]e^{-j\Omega t}\right\}\end{aligned} \tag{19}$$

3.4 Magnetic Force and Torque Densities

Steady state flow is assumed as the fluid responds to the time average (< >) component of both the force and torque density terms in Eq. 4 and Eq. 5. These are given as

$$\langle\mathbf{F}\rangle = \frac{\mu_0}{2}\mathrm{Re}\left[(\widehat{\mathbf{M}}\cdot\nabla)\widehat{\mathbf{H}}^*\right] \tag{20}$$

$$\langle\mathbf{T}\rangle = \frac{\mu_0}{2}\mathrm{Re}\left[\widehat{\mathbf{M}}\times\widehat{\mathbf{H}}^*\right] \tag{21}$$

where * represents the complex conjugate. The time average components of the magnetic force density can then be determined to be

$$\langle \mathrm{F_x}\rangle = -\frac{\mathrm{d}}{\mathrm{dx}}\left(\frac{\mu_0}{4}\left|\widehat{M}_x\right|^2\right), \langle \mathrm{F_z}\rangle = 0 \tag{22}$$

and similarly the torque density

$$\langle \mathrm{T_y}\rangle = \frac{1}{2}\mathrm{Re}\left[\widehat{M}_z\hat{B}_x^{\,*} - \mu_0\widehat{M}_x^{\,*}(\widehat{M}_z + \widehat{H}_z)\right] \tag{23}$$

Simplifying Eqns 6 & 7 and substituting the torque and force densities of Eqns 22 & 23 gives

$$0 = -\frac{\partial p'}{\partial z} + 2\zeta\frac{d\omega_y}{dx} + (\zeta + \eta)\frac{\mathrm{d}^2 v_z}{\mathrm{dx}^2} \tag{24}$$

$$0 = \langle \mathrm{T_y}\rangle - 2\zeta\left(\frac{\mathrm{d}v_z}{\mathrm{dx}} + 2\omega_y\right) + \eta'\frac{\mathrm{d}^2\omega_y}{\mathrm{dx}^2} \tag{25}$$

where p' is a modified pressure that includes pressure, <F_x> and gravitational effects

$$p' = p + \frac{\mu_0}{4}\left|\widehat{M}_x\right|^2 + \rho g x \tag{26}$$

3.5 Normalized general equations

The parameters are expressed in dimensionless form indicated by tildes, given in Eq. 27 with time normalized to the magnetic relaxation time τ, space normalized to the duct spacing d, and magnetic field quantities normalized to a nominal magnetic field strength H_0.

$$\begin{aligned}&\tilde{\Omega} = \Omega\tau, \tilde{\boldsymbol{H}} = \frac{\widehat{\boldsymbol{H}}}{H_0}, \tilde{\boldsymbol{M}} = \frac{\widehat{\boldsymbol{M}}}{H_0}, \tilde{\boldsymbol{B}} = \frac{\widehat{\boldsymbol{B}}}{\mu_0 H_0}, \tilde{x} = \frac{x}{d}\\ &\tilde{v_z} = \frac{v_z\tau}{d}, \tilde{\omega}_y = \omega_y\tau, \tilde{T}_y = \frac{T_y}{\mu_0 {H_0}^2}, \tilde{\eta} = \frac{2\eta}{\mu_0 {H_0}^2\tau}\\ &\tilde{\eta}' = \frac{\eta'}{\mu_0 {H_0}^2\tau d^2}, \tilde{\zeta} = \frac{2\zeta}{\mu_0 {H_0}^2\tau}, \frac{\partial\tilde{p}'}{\partial\tilde{z}} = \frac{d}{\mu_0 {H_0}^2}\frac{\partial p'}{\partial z}\end{aligned} \tag{27}$$

The coupled dimensionless flow and spin velocity equations are then given as

$$0 = -\frac{\partial\tilde{p}'}{\partial\tilde{z}} + \tilde{\zeta}\frac{d\tilde{\omega}_y}{d\tilde{x}} + \frac{1}{2}\left(\tilde{\zeta} + \tilde{\eta}\right)\frac{\mathrm{d}^2\tilde{v}_z}{\mathrm{d}\tilde{\mathrm{x}}^2} \tag{28}$$

$$0 = \langle\tilde{\mathrm{T}}_\mathrm{y}\rangle - \tilde{\zeta}\left(\frac{\mathrm{d}\tilde{v_z}}{\mathrm{d}\tilde{\mathrm{x}}} + 2\tilde{\omega}_y\right) + \tilde{\eta}'\frac{\mathrm{d}^2\tilde{\omega}_y}{\mathrm{d}\tilde{\mathrm{x}}^2} \tag{29}$$

where

$$\langle\tilde{\mathrm{T}}_\mathrm{y}\rangle = \frac{1}{2}\mathrm{Re}\left[\tilde{M}_z\tilde{B}_x^{\,*} - \tilde{M}_x^{\,*}(\tilde{M}_z + \tilde{H}_z)\right] \tag{30}$$

and magnetization derived in Eqns 17 & 18 given by

$$\tilde{M}_x = \frac{\chi_0\left[\tilde{H}_z\tilde{\omega}_y + (j\tilde{\Omega} + 1)\tilde{B}_x\right]}{\left[\tilde{\omega}_y^{\,2} + (j\tilde{\Omega} + 1)(j\tilde{\Omega} + 1 + \chi_0)\right]} \tag{31}$$

$$\tilde{M}_z = \frac{\chi_0\left[(j\tilde{\Omega} + 1 + \chi_0)\tilde{H}_z - \tilde{\omega}_y\tilde{B}_x\right]}{\left[\tilde{\omega}_y^{\,2} + (j\tilde{\Omega} + 1)(j\tilde{\Omega} + 1 + \chi_0)\right]} \tag{32}$$

Substituting Eqns 31 & 32 into Eq. 30 gives the exact torque density expression as

$$\langle \tilde{T}_y \rangle = \frac{\chi_0}{2}\left[\begin{array}{c} -\tilde{\omega}_y\left[\begin{array}{c}|\tilde{H}_z|^2[\tilde{\omega}_y{}^2 - \tilde{\Omega}^2 + (1+\chi_0)^2] + \\ |\tilde{B}_x|^2[\tilde{\omega}_y{}^2 - \tilde{\Omega}^2 + 1]\end{array}\right] \\ +2\,\mathrm{Re}\left[\left[\begin{array}{c}\chi_0(\tilde{\omega}_y{}^2 - \tilde{\Omega}^2) \\ +j\tilde{\Omega}(\tilde{\omega}_y{}^2 - \tilde{\Omega}^2 - 1 - \chi_0)\end{array}\right][\tilde{H}_z\tilde{B}_x{}^*]\right] \end{array}\right] \Big/ \left[[\tilde{\omega}_y{}^2 - \tilde{\Omega}^2 + 1 + \chi_0]^2 + (2+\chi_0)^2\tilde{\Omega}^2\right] \quad (33)$$

Zahn [6] simplifies this expression by linearizing the torque in the limit of small $\tilde{\omega}_y$ and is given by the form

$$\lim_{\tilde{\omega}_y \ll 1} \langle \tilde{T}_y \rangle \approx \tilde{T}_0 + \alpha\tilde{\omega}_y \quad (34)$$

where

$$\langle \tilde{T}_0 \rangle = \frac{-\chi_0 \mathrm{Re}\left[[\chi_0\tilde{\Omega}^2 + j\tilde{\Omega}(\tilde{\Omega}^2 + 1 + \chi_0)][\tilde{H}_z\tilde{B}_x{}^*]\right]}{(\tilde{\Omega}^2 + 1 + \chi_0)^2 + \tilde{\Omega}^2\chi_0{}^2} \quad (35)$$

$$\langle \alpha \rangle = \frac{\chi_0}{2}\frac{\left[|\tilde{B}_x|^2(\tilde{\Omega}^2 - 1) + |\tilde{H}_z|^2[\tilde{\Omega}^2 - (1+\chi_0)^2]\right]}{(\tilde{\Omega}^2 + 1 + \chi_0)^2 + \tilde{\Omega}^2\chi_0{}^2} \quad (36)$$

3.6 Boundary Conditions

For Eq. 28 the no slip velocity boundary condition was implemented. For Eq. 29, the boundary condition on spin velocity $\tilde{\omega}_y$ was set to 0 if $\tilde{\eta}' \neq 0$, otherwise if $\tilde{\eta}' = 0$ no boundary condition was implemented on spin velocity $\tilde{\omega}_y$. These boundary conditions for $\tilde{\eta}' \neq 0$ are

$$\begin{array}{c}\tilde{v_z}(\tilde{x}=0) = 0 \\ \tilde{v_z}(\tilde{x}=1) = 0 \\ \tilde{\omega}_y(\tilde{x}=0) = 0 \text{ (only if } \tilde{\eta}' \neq 0) \\ \tilde{\omega}_y(\tilde{x}=1) = 0 \text{(only if } \tilde{\eta}' \neq 0)\end{array} \quad (37)$$

4. Modeling

4.1 Model Parameters

The results of Zahn and Greer [6] were first replicated with parameters taken from their paper such as χ_0=1, $\tilde{\Omega}$=1, $\tilde{\zeta}$=$\tilde{\eta}$=1,$\frac{d\tilde{p}'}{dz}$=0.00001. Pioch, in her analytical results [8-10], obtained kinks in her distribution of flow and spin velocities with certain parameters. These parameters were used to verify her results using COMSOL Multiphysics 3.5a.

4.2 Using COMSOL Multiphysics 3.5a

The 2D steady state *Incompressible Navier Stokes* module was used to represent the conservation of linear momentum equation in Eq. 28. The subdomain and boundary settings used in COMSOL are listed in Table 1 and Table 2 respectively.

COMSOL quantities	Eq. 28
ρ	0
η	$\frac{1}{2}(\tilde{\zeta} + \tilde{\eta})$
F_x	$\tilde{\zeta}\frac{d\tilde{\omega}_y}{d\tilde{x}}$
F_y	0

Table 1. Coefficients for subdomain settings of the 2D Navier Stokes module in COMSOL 3.5a representing the linear momentum conservation equation of Eq. 28.

Boundary Conditions	COMSOL quantities
Inlet Left wall	Pressure, No viscous Stress $p_0 = -\tilde{p}'$ such that $\frac{\partial\tilde{p}'}{\partial\tilde{z}} > 0$ is obtained
Outlet Right wall	Normal Stress f_0=0
Other Duct Walls	No slip $\tilde{v_z} = 0$

Table 2. Coefficients for boundary settings of the 2D Navier Stokes module in COMSOL 3.5a representing the linear momentum conservation equation of Eq. 28.

A *General PDE* module was used to represent the conservation of angular momentum equation in Eq. 29. The subdomain settings used are listed in Table 3. The boundary settings used are listed in Table 4 for either case, $\tilde{\eta}' = 0$ or $\tilde{\eta}' \neq 0$.

COMSOL quantities	Eq. 29
Γ	0,0
F	$\langle \tilde{T}_y \rangle - \tilde{\zeta}\left(\frac{d\tilde{v_z}}{d\tilde{x}} + 2\tilde{\omega}_y\right) + \tilde{\eta}'\frac{d^2\tilde{\omega}_y}{d\tilde{x}^2}$
e_a	0
d_a	0

Table 3. Coefficients for subdomain settings of the 2D General PDE module in COMSOL 3.5a representing the angular momentum conservation equation of Eq. 29.

Boundary Conditions	COMSOL quantities
All walls (if $\tilde{\eta}'\neq 0$)	Dirichlet boundary condition R= $-\tilde{\omega}_y$, G=0
All walls (if $\tilde{\eta}'=0$)	Neumann boundary condition G=0

Table 4. Coefficients for boundary settings of the 2D General PDE module in COMSOL 3.5a representing the linear momentum conservation equation of Eq. 29.

The ferrofluid magnetization in Eqns 31 & 32 was implemented using the 2D *Perpendicular Induction Currents, Vector Potential* module with subdomain settings listed in Table 5. A magnetic field boundary condition was applied which poses a subtlety. The magnetic field in the vertical direction, $\tilde{H}_x(x)$, and not the constant magnetic flux $\tilde{B}_x$, has to be implemented using the relationship in Eq. 16 as described in Table 6 (note the normalization).

COMSOL quantities	Eq. 31 & 32
Magnetization **M**	$\frac{\chi_0\left[\tilde{H}_z\tilde{\omega}_y+(j\tilde{\Omega}+1)\tilde{B}_x\right]}{\left[\tilde{\omega}_y{}^2+(j\tilde{\Omega}+1)(j\tilde{\Omega}+1+\chi_0)\right]}$, $\frac{\chi_0\left[(j\tilde{\Omega}+1+\chi_0)\tilde{H}_z-\tilde{\omega}_y\tilde{B}_x\right]}{\left[\tilde{\omega}_y{}^2+(j\tilde{\Omega}+1)(j\tilde{\Omega}+1+\chi_0)\right]}$

Table 5. Coefficients for subdomain settings of the 2D *Perpendicular Induction Currents, Vector Potential* module in COMSOL 3.5a representing the magnetization vectors of Eq. 31 & 32.

Boundary Conditions	COMSOL quantities
All Walls	Magnetic Field $H_0=\tilde{H}_z$, $\tilde{H}_x=\tilde{B}_x-\tilde{M}_x$

Table 6. Coefficients for subdomain settings of the 2D *Perpendicular Induction Currents, Vector Potential* module in COMSOL 3.5a representing the magnetization vectors of Eq. 31 & 32.

All modules use stationary analysis except for the *2D Perpendicular Induction Currents, Vector Potential* module. This module was made *transient* so that the magnetic field boundary conditions are slowly ramped up in time, using COMSOL's ramp (*flc2hs*) function, to aid convergence.

4.3 Using Mathematica

The boundary value problem described by Eqns 28-32 and Eq. 37 was solved using the *shooting method* in Mathematica 8.0. Solutions were obtained using the complete torque equation in Eq. 33, as well as, the linearized torque equation in Eq. 34-36**.**

5. Results and Discussion

Many cases were investigated and the most interesting cases will be discussed in this work.

For flows with non-zero spin viscosity ($\tilde{\eta}'\neq 0$), the velocity flow profile in the duct is illustrated in Figure 3 and Figure 4 for an imposed, relatively weak, rotating field ($\tilde{B}_x$=0.1, $\tilde{H}_z$=0.1j). The spin velocity profile with zero spin velocity boundary conditions ($\tilde{\omega}_y$=0) at the boundaries can be seen in Figure 5. The complete and linearized torque solutions are identical for such a low field strengths since the spin velocity approximation ($\tilde{\omega}_y$<<1) holds. There is some deviation between COMSOL results and the results obtained in Mathematica but overall good agreement between the two.

If the magnetic field/flux strength is increased, the small spin limit approximation for the linearized torque (Eqns. 34-36) equation does not hold. As a result, there would be a significant difference in the effects of the complete (Eq. 33) and linearized torque equations. This effect is illustrated, with good agreement between COMSOL and Mathematica complete torque results, in the flow and spin velocity plots of Figure 6 and Figure 7 for a strong rotating field ($\tilde{B}_x$=10, $\tilde{H}_z$=j). The spin velocity magnitude in Figure 7 also illustrates that the small spin velocity limit ($\tilde{\omega}_y$<<1) does not hold.

Figure 6 and Figure 7 are also examples of flow profiles simulated with zero spin viscosity ($\tilde{\eta}'$=0). The resulting spin velocity profile is constant throughout the duct due to no boundary condition (Figure 7). The velocity profile in the duct can be seen in Figure 8.

Pioch [8-10] calculated for certain parameters kinks in flow and spin velocity distributions would be obtained. Simulations using these parameters were done giving identical results between COMSOL and Mathematica as seen in Figure 9.

Figure 3. Velocity profile with parameters χ_0=1, $\tilde{\Omega}$=1, $\tilde{\zeta}$=$\tilde{\eta}$=1, $\frac{d\tilde{p}'}{dz}$=0.00001 for non-zero spin viscosity condition ($\tilde{\eta}'$=0.01).

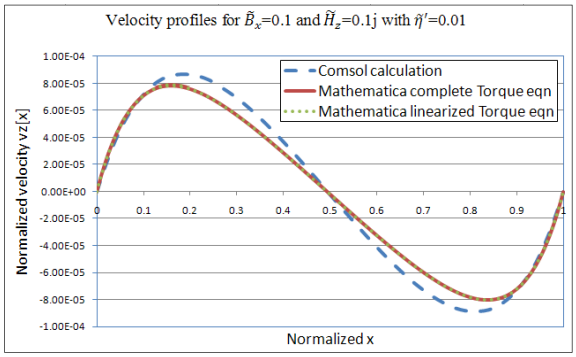

Figure 4. Normalized flow velocity $\tilde{v_z}(\tilde{x})$ for an imposed rotating normalized rotating field with χ_0=1, $\tilde{\Omega}$=1, $\tilde{\zeta}$=$\tilde{\eta}$=1, $\frac{d\tilde{p}\prime}{dz}$ =0.00001, $\tilde{B}_x$=0.1, $\tilde{H}_z$=0.1j and non-zero spin viscosity condition ($\tilde{\eta}'$=0.01).

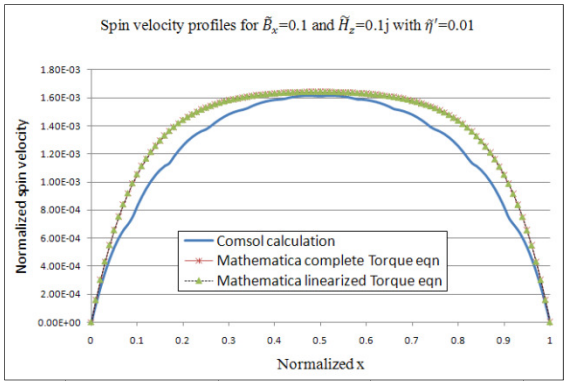

Figure 5. Normalized flow velocity $\tilde{\omega}_y(\tilde{x})$ for an imposed rotating normalized rotating field with χ_0=1, $\tilde{\Omega}$=1, $\tilde{\zeta}$=$\tilde{\eta}$=1, $\frac{d\tilde{p}\prime}{dz}$ =0.00001, $\tilde{B}_x$=0.1, $\tilde{H}_z$=0.1j and non-zero spin viscosity condition ($\tilde{\eta}'$=0.01).

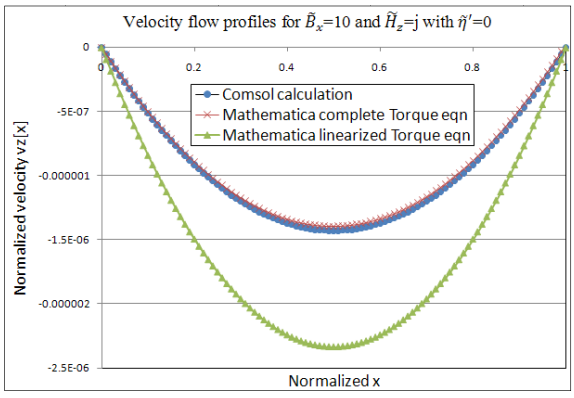

Figure 6. Normalized flow velocity $\tilde{v_z}(\tilde{x})$ for an imposed rotating normalized rotating field with $\tilde{B}_x$=10, $\tilde{H}_z$=j and zero spin viscosity condition ($\tilde{\eta}'$=0) and χ_0=1, $\tilde{\Omega}$=1, $\tilde{\zeta}$=$\tilde{\eta}$=1, $\frac{d\tilde{p}\prime}{dz}$ =0.00001. The linearized torque equation gives a significantly different result than the solution obtained with the complete torque equation.

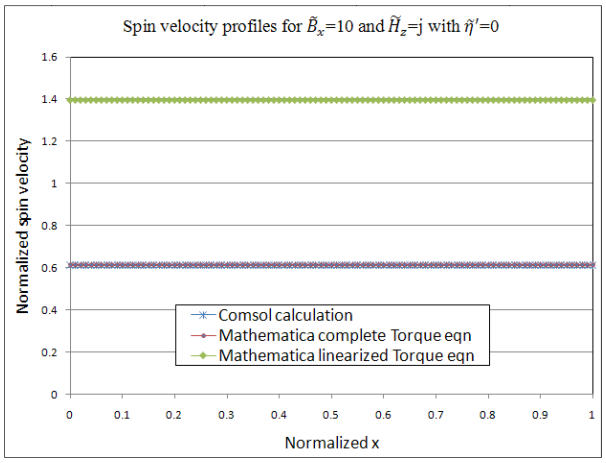

Figure 7. Normalized spin velocity $\tilde{\omega}_y(\tilde{x})$ for an imposed rotating normalized rotating field with $\tilde{B}_x$=10, $\tilde{H}_z$=j and zero spin viscosity condition ($\tilde{\eta}'$=0) and χ_0=1, $\tilde{\Omega}$=1, $\tilde{\zeta}$=$\tilde{\eta}$=1, $\frac{d\tilde{p}\prime}{dz}$ =0.00001. The linearized torque equation gives a significantly different result than the solution obtained with the complete torque equation.

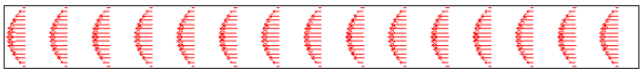

Figure 8. Velocity profile with parameters χ_0=1, $\tilde{\Omega}$=1, $\tilde{\zeta}$=$\tilde{\eta}$=1, $\frac{d\tilde{p}\prime}{dz}$ =0.00001 for zero spin viscosity condition ($\tilde{\eta}'$=0).

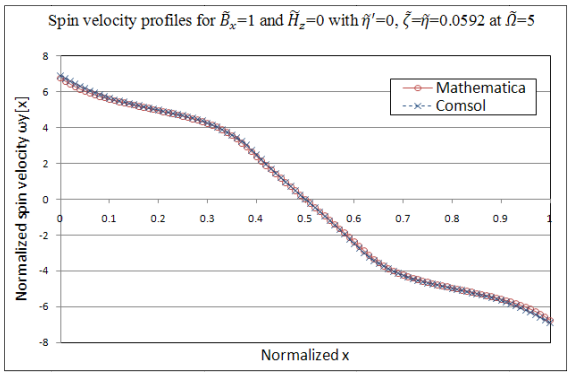

Figure 9. Normalized spin velocity $\tilde{\omega}_y(\tilde{x})$ for an imposed rotating normalized rotating field with $\tilde{B}_x$=1, $\tilde{H}_z$=0 and zero spin viscosity condition ($\tilde{\eta}'$=0) and χ_0=1, $\tilde{\Omega}$=5, $\tilde{\zeta}$=$\tilde{\eta}$=0.0592, $\frac{d\tilde{p}\prime}{dz}$ =1. Pioch's kinks [8-10] are replicated in COMSOL with good agreement to analytical solutions in Mathematica.

6. Conclusions

Ferrohydrodynamic flows are difficult to analyze due to the coupling of five vector equations. These constitute of the linear and angular momentum conservation equations along with Ampere's law with no free current ($\nabla \times \mathbf{H} = 0$), Gauss's law for magnetic flux density ($\nabla \cdot \mathbf{B} = 0$) and the ferrofluid magnetic relaxation equation.

Ferrofluid pumping in a planar geometry, subjected to tangential and perpendicular magnetic fields, is a well posed problem with analytical solutions. This work highlights the use of a multiphysics finite element package such as COMSOL Multiphysics in replicating previously obtained Mathematica results with very good agreement between the two.

7. Acknowledgements

The authors would like to acknowledge the Binational Science Foundation for partial financial support for this project (BSF Grant No. 20004081).

8. References

[1] S. Khushrushahi and M. Zahn, "Understanding ferrofluid spin-up flows in rotating uniform magnetic fields," in *Proceedings of the COMSOL Conference*, Boston, 2010.

[2] S. Khushrushahi and M. Zahn, "Ultrasound velocimetry of ferrofluid spin-up flow measurements using a spherical coil assembly to impose a uniform rotating magnetic field," *Journal of Magnetism and Magnetic Materials,* vol. 323, pp. 1302-1308, 2011.

[3] S. Khushrushahi and M. Zahn, "Ultrasound velocimetry of ferrofluid spin-up flow measurements using a spherical coil assembly to impose a uniform rotating magnetic field," presented at the 12th International Conference on Magnetic Fluids, Sendai, Japan, 2010.

[4] S. Khushrushahi, "Ferrofluid Spin-up Flows in Uniform and Non-uniform Rotating Magnetic Fields," PhD, Dept. of Electrical Engineering and Computer Science, Massachusetts Institute of Technology, Cambridge, 2010.

[5] B. Finlayson, "Modeling a Ferrofluid in a Rotating Magnetic Field," presented at the COMSOL Users' Conference, Boston, 2007.

[6] M. Zahn and D. Greer, "Ferrohydrodynamic pumping in spatially uniform sinusoidally time-varying magnetic fields," *Journal of Magnetism and Magnetic Materials,* vol. 149, pp. 165-173, 1995.

[7] X. He, "Ferrohydrodynamic flows in uniform and non-uniform rotating magnetic fields," Ph.D thesis, Dept. of Electrical Engineering and Computer Science, Massachusetts Institute of Technology, Cambridge, MA, 2006.

[8] M. Zahn and L. Pioch, "Ferrofluid flows in AC and traveling wave magnetic fields with effective positive, zero or negative dynamic viscosity," *J. Magn. Magn. Mater.,* vol. 201, p. 144, 1999.

[9] M. Zahn and L. L. Pioch, "Magnetizable fluid behaviour with effective positive, zero or negative dynamic viscosity," *Indian Journal of Engineering & Materials Sciences,* vol. 5, pp. 400-410, 1998.

[10] L. L. V. Pioch, "Ferrofluid flow & spin profiles for positive and negative effective viscosities," Masters of Engineering, Dept. of Electrical Engineering and Computer Science, Massachusetts Institute of Technology, 1997.

[11] R. E. Rosensweig, *Ferrohydrodynamics*: Dover Publications, 1997.

[12] M. I. Shliomis, "Effective viscosity of magnetic suspensions," *Soviet Physics JETP,* vol. 34, pp. 1291-1294, 1972.